




Article

Preparation of Polydimethylsiloxane-Modified Waterborne Polyurethane Coatings for Marine Applications

Min-Gu Kim ¹, Kyoung-Il Jo ¹, Eunji Kim ², Jae-Hyung Park ¹, Jae-Wang Ko ^{1,*} and Jin Hong Lee ^{2,*}

¹ Industry Fiber Laboratory, Korea Institute of Footwear & Leather Technology (KIFLT), Busan 47454, Korea; kimmingu95@pusan.ac.kr (M.-G.K.); kyeoungil@gmail.com (K.-I.J.); jhpark@kiflt.re.kr (J.-H.P.)

² School of Chemical Engineering, Pusan National University, Busan 46241, Korea; eunjikim@pusan.ac.kr

* Correspondence: jwko@kiflt.re.kr (J.-W.K.); jinhong.lee@pusan.ac.kr (J.H.L.)

Abstract: A series of waterborne polyurethane dispersions (WPU) modified with hydroxyl-terminated polydimethylsiloxane (PDMS) were prepared by incorporating PDMS into the soft segments of polyurethane chains. The structural characteristics of the prepared samples were analyzed by Fourier transform infrared spectroscopy (FTIR), X-ray diffraction (XRD), X-ray photoelectron spectroscopy (XPS), and particle size analysis (PSA). The effect of PDMS content on the thermal and mechanical properties of PDMS-modified waterborne polyurethanes (PS-WPU) was investigated. In addition, the water resistance and dimensional stability of the PS-WPU were investigated by measuring its water absorption ratio and water contact angle along with universal testing machine measurements.

Keywords: waterborne polyurethanes; polyurethane coatings; polydimethylsiloxanes; hydrophobicity; marine applications



Citation: Kim, M.-G.; Jo, K.-I.; Kim, E.; Park, J.-H.; Ko, J.-W.; Lee, J.H. Preparation of Polydimethylsiloxane-Modified Waterborne Polyurethane Coatings for Marine Applications. *Polymers* **2021**, *13*, 4283. <https://doi.org/10.3390/polym13244283>

Received: 2 November 2021

Accepted: 2 December 2021

Published: 7 December 2021

Publisher's Note: MDPI stays neutral with regard to jurisdictional claims in published maps and institutional affiliations.



Copyright: © 2021 by the authors. Licensee MDPI, Basel, Switzerland. This article is an open access article distributed under the terms and conditions of the Creative Commons Attribution (CC BY) license (<https://creativecommons.org/licenses/by/4.0/>).

1. Introduction

Polyurethane (PU), a polymer joined by urethane bonds, is produced by the reaction of polyols with isocyanates. Currently, PUs are one of the most commonly used materials in various applications such as coatings [1,2], adhesives [3,4], foams [5,6], and elastomers [7,8]. The properties of PU are dependent on the type of polyols and isocyanates used, and the soft segment of PU is formed from a polyol, while the hard segment is composed of an isocyanate and a chain extender.

In recent years, with increasingly strict regulations for volatile organic compounds, waterborne polyurethanes (WPU), which utilize water as a dispersion medium, have received significant attention [9]. WPU are synthesized by introducing hydrophilic segments or ionic groups, which act as emulsifiers, into the molecular chains of the polymers [10]. WPU have been applied in a wide range of adhesives and coatings for textile, plastic, metal, and offshore structures owing to their tunable properties, which can be controlled by the proportion of soft and hard segments [9,11]. However, their low resistance in water and solvents, apart from limited thermal stability and mechanical properties, needs to be improved in order to replace solvent-based PUs.

Considerable efforts have been devoted into overcoming these problems, including the introduction of a network structure enabled by a crosslinking reaction of epoxy [12] and acrylic groups [13,14], blending WPU with different polymers to form interpenetrating networks (IPNs) [15], modifying the chemical structures of WPU with nanoparticles [16,17], and copolymerization [18,19]. Another promising approach is the use of polydimethylsiloxane (PDMS) because of its advantageous properties, such as high thermal stability, biocompatibility, flexibility, water resistance, and low surface energy [20–25]. Vlad et al. reported that IPNs prepared by the combination of castor-oil-based PUs and PDMS provide enhanced mechanical properties. However, the IPNs exhibited significant phase separation due to a large difference in the solubility parameter between the PU network and PDMS network [26]. Compared with solvent-based PUs, WPU containing ionic moieties or

hydrophilic segments are more polar; this results in a large polarity difference between WPU and PDMS and their poor compatibility. Hence, research has largely focused on chemical modifications to increase the compatibility of WPU and PDMS [27,28].

In this study, different amounts of hydroxyl-terminated PDMS were incorporated into the molecular chains of WPU as soft segments to investigate the effects of the PDMS content on the mechanical and thermal properties of PDMS-modified PU. Analytical results revealed that an increase in the PDMS content resulted in improved thermal stability, elongation properties, and water resistance, while decreasing the tensile strength. These findings are important for understanding the potential marine applications of PDMS-modified PUs.

2. Materials and Methods

2.1. Materials

Polytetramethylene ether glycol (PTMG, Aldrich, St. Louis, MO, USA) ($M_n = 2000 \text{ g mol}^{-1}$), hydroxyl-terminated PDMS (Aldrich) ($M_n = 4200 \text{ g mol}^{-1}$), isophorone diisocyanate (IPDI, Aldrich; 98%), 2,2-bis(hydroxymethyl) propionic acid (DMPA, Aldrich; 98%), dibutyltin dilaurate (DBTDL, Aldrich; 95%), triethylamine (TEA, Samchun Chemical Co., Ltd. Pingze, Korea; 99%), and ethylenediamine (EDA, Samchun Chemical Co., Ltd.; 99%) were used as received.

2.2. Preparation of PS-WPU

A series of WPU samples with different PDMS contents (0, 5, 10, 15 and 20%) were synthesized using the prepolymer method as follows: PTMG, PDMS, and DMPA were first placed in a three-necked glass reactor equipped with a physical stirrer, dropping funnel, and a screw tube cooler. The mixture was then stirred at 80 °C. After 1 h, IPDI and DBTDL were added dropwise to the reactor. The reaction was carried out at 80 °C for 3 h to obtain the NCO-terminated prepolymer. During the reaction, acetone was added to adjust the viscosity of the solution. After reaction completion, the solution was cooled to 40 °C, and then TEA was added to neutralize the carboxyl groups of PU. After 1 h of neutralization, distilled water was added with vigorous stirring for 1 h, and then EDA was added for chain extension for another 1 h. Finally, acetone was removed under vacuum to obtain the WPU dispersion. The WPU films were prepared by casting the WPU dispersion into a glass mold and drying at room temperature until all the solvents had evaporated. The sample designations and compositions are summarized in Table 1, and the reaction process is illustrated in Scheme 1.

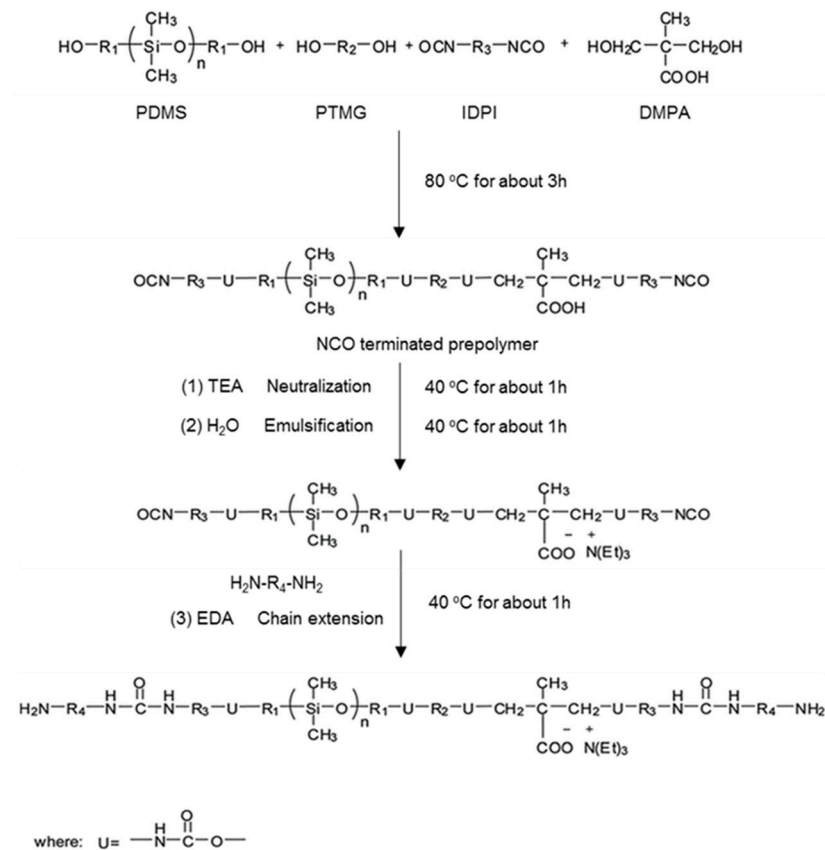
Table 1. Composition of PS-WPU samples.

Samples	Composition (mol)					
	PDMS	PTMG	DMPA	IPDI	TEA	EDA
PS-WPU 1	0	0.033	0.067	0.12	0.067	0.02
PS-WPU 2	0.00165	0.03135	0.067	0.12	0.067	0.02
PS-WPU 3	0.0033	0.0297	0.067	0.12	0.067	0.02
PS-WPU 4	0.00495	0.02805	0.067	0.12	0.067	0.02
PS-WPU 5	0.0066	0.0264	0.067	0.12	0.067	0.02

2.3. Characterization

Fourier-transform infrared (FTIR) spectra of the samples were analyzed using an FTIR spectrometer (JASCO Co., FT/IR-6200, Tokyo, Japan) using attenuated total reflection (ATR) method. The spectra were recorded in the range of 4000–400 cm^{-1} at a resolution of 4 cm^{-1} , and each sample was scanned 64 times.

The particle sizes of the samples were determined using a particle size analyzer (PSA) (Malvern Panalytical, Mastersizer 3000, Malvern, UK). The samples were diluted to a concentration of 0.01% using deionized water (D.W).



Scheme 1. Preparation of PS-WPU.

X-ray diffraction (XRD) patterns were obtained using an X-ray diffractometer (Philips, X'pert 3, Eindhoven, Netherlands) with Cu-K α radiation ($\lambda = 1.54060 \text{ \AA}$) at 40 kV and 30 mA. The angle was between 20° and 40° with a step size of 0.01°.

Qualitative and quantitative information on the surface elemental compositions of the samples were obtained via X-ray photoelectron spectroscopy (XPS, Thermo Fisher Scientific, Waltham, MA, USA) with Al K α achromatic X-ray. The spectra were recorded in the range of 0–1300 eV under 90° take-off angles.

Dynamic mechanical analysis (DMA) was conducted using a DMA instrument (TA Instruments, DMA 850, New Castle, DE, USA). The temperature was in the range of –100 °C to 100 °C, with a heating rate of 5 °C/min at an oscillating frequency of 1 Hz.

Thermogravimetric analysis (TGA) and derivative thermogravimetric (DTG) analysis were conducted using a thermal analyzer (TA Instruments, TGA Q500, New Castle, DE, USA) at a heating rate of 10 °C/min in a nitrogen atmosphere, with temperatures in the range of 100 °C to 800 °C.

The tensile properties were measured using a universal testing machine (Instron Co., Instron 3345, Canton, OH, USA) at a crosshead speed of 50 mm/min at room temperature and –60 °C. The mechanical test on each dumbbell-shaped sample was conducted five times, and the average value was calculated according to the ASTM D638.

Water contact angles (WCAs) were measured with a contact angle goniometer (Femto-biomed, Smart Drop Standard, Seongnam, Korea) at room temperature with water droplets (deionized water (D.W) and seawater (S.W)). Each sample was analyzed thrice at three different locations, and the average value of the contact angle was calculated. The surface free energy was calculated by inputting the value of the contact angle to the surface energy calculation software.

To measure the swelling in water, the films were immersed in water (D.W and S.W) at 25 °C. The water swelling properties were calculated from the differences in the mass of the samples using the following equation:

$$\text{Swelling ratio} = \frac{100(W - W_0)}{W_0}$$

where W_0 and W represent the initial and final (after water swelling) film weights, respectively.

3. Results and Discussion

3.1. FTIR Analysis

The chemical structures of the PS-WPU samples are investigated by FTIR spectroscopy, as shown in Figure 1. All the samples indicate the absorption peaks of typical PU at 1530 cm^{-1} (–NH bending in urethane), 1717 cm^{-1} (–C=O stretching in urethane), 1160 cm^{-1} (C–O–C ether group) and $2923\text{--}2850\text{ cm}^{-1}$ (C–H symmetric and asymmetric stretching of CH_2 group, respectively) [29]. The absorption peaks near 3480 cm^{-1} and 3320 cm^{-1} indicate free NH stretching and hydrogen-bonded NH stretching, respectively [30]. The absence of an NCO peak at 2270 cm^{-1} in all the samples indicates the complete reaction of the NCO group. Furthermore, except for PS-WPU 1, all the remaining PS-WPU samples indicate the characteristic absorption peaks of Si– CH_3 at 1261 cm^{-1} (Si– CH_3 deformation), Si–O–Si at 1023 cm^{-1} (Si–O stretching), and Si– CH_3 at $806\text{--}1010\text{ cm}^{-1}$ (CH_3 rocking and Si–C stretching), which indicates that PDMS was successfully incorporated into WPU [31]. In addition, the intensity of the absorption peak increases with increasing PDMS content.

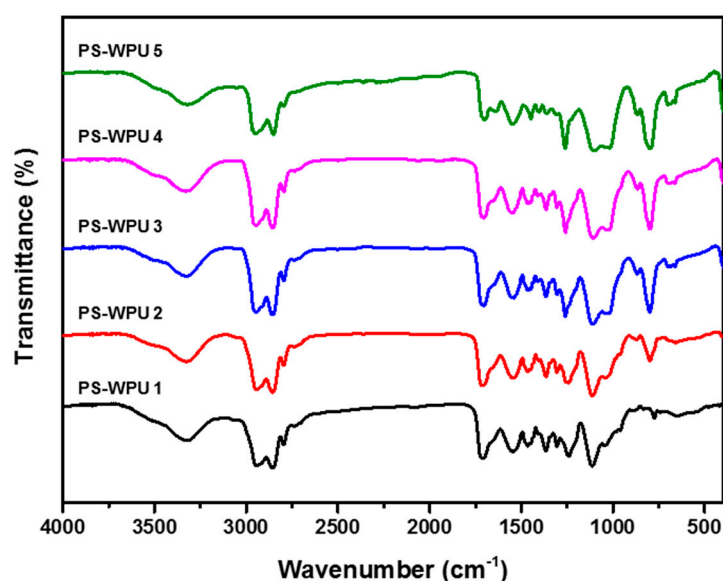


Figure 1. FTIR spectra of PS–WPU samples.

3.2. Particle Size of the PS–WPU Dispersions

Figure 2 and Table 2 present the particle size distribution of the PS-WPU dispersions with different PDMS contents. The average particle size of the PS-WPU dispersions increase with increasing PDMS content from 0.331 to $4.45\text{ }\mu\text{m}$. However, the PS-WPU dispersions exhibited bimodal particle-size distributions. These results may be ascribed to the hydrophobicity of the PDMS chains. During the formation of colloidal particles in the water-based dispersions, the hydrophilic groups and segments tend to be on the outer layers, while the hydrophobic PDMS favored the inner layers. As a result, a higher content of PDMS results in a larger free volume and lower chain packing density in the interior of the colloidal particles, and thus, larger particles [1,32–34]. Furthermore, all the PS-WPU

dispersions showed good stability with no precipitation at room temperature for a period of three months.

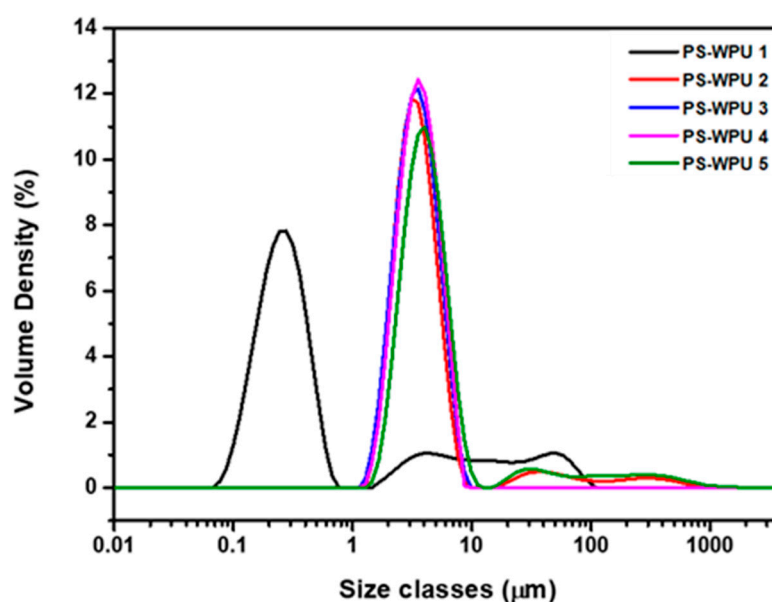


Figure 2. Particle size distribution of PS-WPU samples.

Table 2. Particle size of PS-WPU samples.

Samples	Particle Size (μm)
PS-WPU 1	0.331
PS-WPU 2	3.65
PS-WPU 3	3.70
PS-WPU 4	3.79
PS-WPU 5	4.45

3.3. XRD and XPS Analyses

The crystalline structures of the PS-WPUs were investigated using XRD. As shown in Figure 4, there are no sharp peaks in the diffraction patterns, which indicates the amorphous structures of the PS-WPUs. All the PS-WPU samples show a broad peak centered at $2\theta = 20^\circ$, indicating the typical crystalline nature of PU. The crystallinity of PU is due to the hydrogen bonds that occur in the molecules [35,36]. PDMS exhibits a characteristic amorphous halo at 2θ of 12° [37]. All of the samples, except that of PS-WPU 1, show characteristic peaks corresponding to PDMS, and the peak intensity increases with increasing PDMS content. Furthermore, the diffraction pattern becomes weaker and broader, which indicates that the crystallinity and orientation of the PU chains are disturbed by the addition of PDMS.

The elemental composition of the PS-PU coating surface was investigated using XPS. Figure 3a shows the XPS spectra of PS-WPU 1 observed at binding energies of 284, 399, and 532 eV, which are attributed to C 1s, N 1s, and O 1s, respectively. The PDMS-modified samples (PS-WPU 2, 3, 4, and 5) exhibit strong characteristic Si 2p and Si 2s peaks at 102 and 155 eV, respectively. In addition, as the PDMS content increases, the Si atomic content increases from 0 to 20.85% (Figure 3b and Table 3). The presence of the Si peak and the increase in the atomic concentration of Si atoms indicate the successful incorporation of PDMS, which further confirm the FTIR and XRD results.

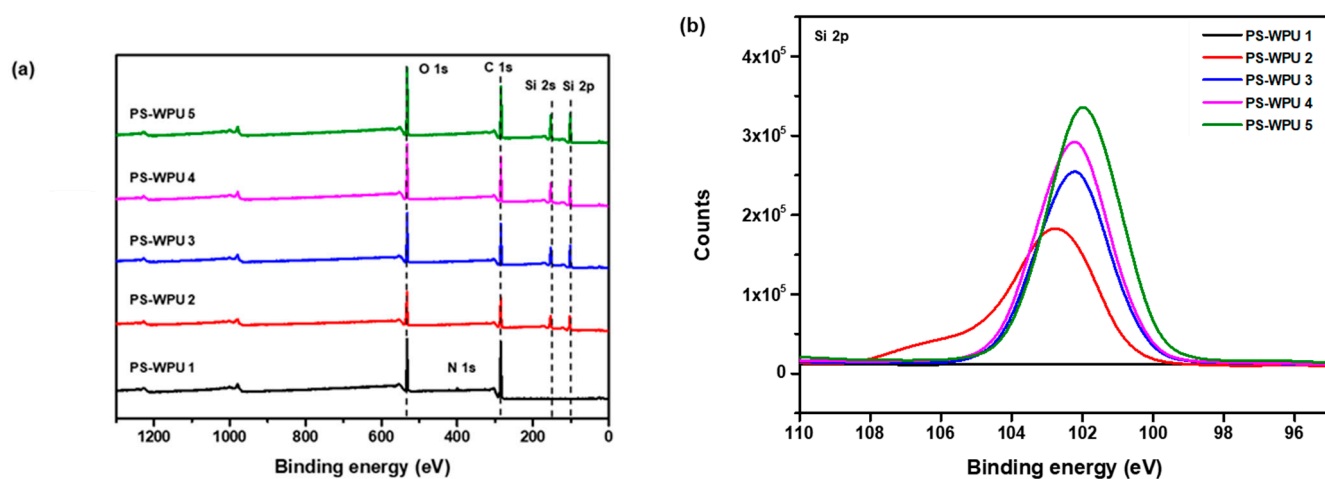


Figure 3. (a) XPS spectra and (b) Si 2p XPS spectra of the PS-WPU samples.

Table 3. Atomic relative concentration of elements in PS-WPU samples.

Samples	O 1s	N 1s	C 1s	Si 2p
PS-WPU 1	45.02	1.82	53.16	0
PS-WPU 2	45.87	0.79	35.57	17.77
PS-WPU 3	46.42	0.62	34.85	18.11
PS-WPU 4	46.82	0.34	33.26	19.58
PS-WPU 5	46.39	0.30	32.46	20.85

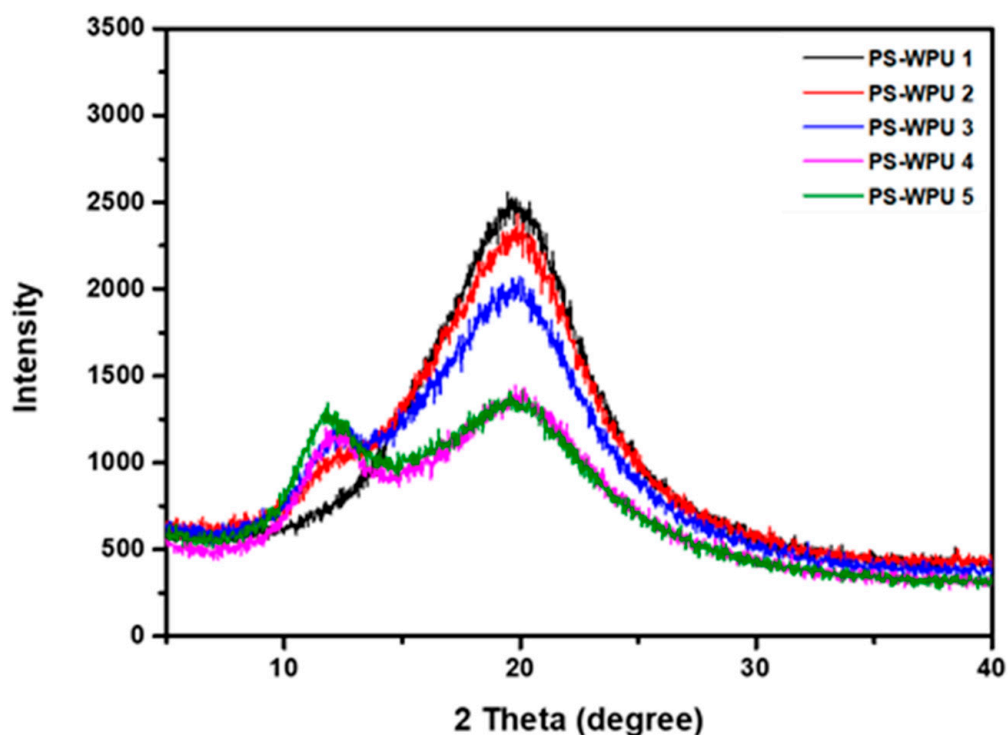


Figure 4. X-ray diffraction patterns of PS-WPU samples.

3.4. DMA Analysis

The viscoelastic properties of the PS-WPU samples were investigated using DMA. Figure 5 presents the storage modulus and damping factor ($\tan \delta$) of the PS-WPUs as a function of temperature. As shown in Figure 5a, the storage modulus curves of all PS-WPU samples decrease abruptly over the temperature range from -100 °C to -35 °C,

which is ascribed to the glass transition in the soft segment [38]. PS-WPU 1 without PDMS exhibits the highest storage modulus, and the storage modulus of the PS-WPU samples decreases with increasing PDMS content. The storage modulus is a measure of material stiffness [39–41], and the incorporation of PDMS into the soft segment of the WPU decreases the stiffness because of the high flexibility of the PDMS. Figure 5b displays the $\tan \delta$ curves, which are directly related to the T_g of the PS-WPU samples. The relatively sharp peak in the $\tan \delta$ curves is ascribed to the primary dispersion (α_a) associated with the glass transition of PU. In this transition temperature region, the storage modulus decreases abruptly, and the micro-Brownian motions of the PU chains become clear in the soft domains [42]. The values of T_g decrease from -59.87°C to -62.49°C with increasing PDMS content because of the enhanced motion of PDMS chains.

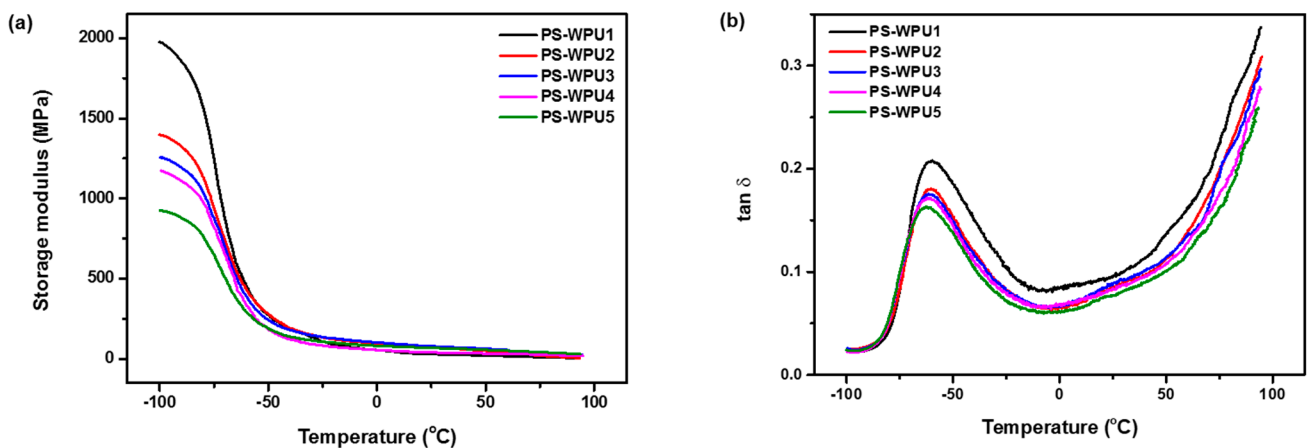


Figure 5. Temperature dependence of (a) storage modulus and (b) $\tan \delta$ of PS-WPU samples.

3.5. TGA and DTG Analyses

To investigate the effect of PDMS on the thermal stability, TGA and DTG analyses were carried out. The results are shown in Figure 6. The characteristic degradation temperatures associated with the thermal degradation are summarized in Table 4. All the PS-WPU samples exhibit similar thermal decomposition behaviors. The slight weight loss before 200°C is caused by the volatilization of solvents in the PS-WPU film. The temperature at which 10% weight loss occurs ($T_{10\%}$) and the mid-point temperature of the weight loss ($T_{50\%}$) are employed to determine the thermal stability of the PS-WPU films, as shown in Table 4. Both the weight loss temperatures, $T_{10\%}$ and $T_{50\%}$, increase with increasing PDMS content. The improvement in thermal stability indicates that PDMS plays an important role in preventing the decomposition of the main chain of WPU. This improved stability can be attributed to the higher energy of the Si–O bond ($\sim 460\text{ kJ/mol}$) compared to the energies of the C–C and C–O bonds ($\sim 345\text{ kJ/mol}$) [43,44].

According to the TGA and DTG curves, all the PS-WPU samples exhibit a three-step degradation profile. The first degradation step from 250°C to 350°C is related to the decomposition of the hard segment of PU, since the C–N bond breaks more easily than the C–O and C–C bonds [45,46]. The second degradation step at around 400°C is due to the scission of the soft segment. The third degradation step above 500°C may correspond to the depolymerization of residual components [47]. These results indicate that increasing the PDMS content improves the thermal stability of the PS-WPU samples.

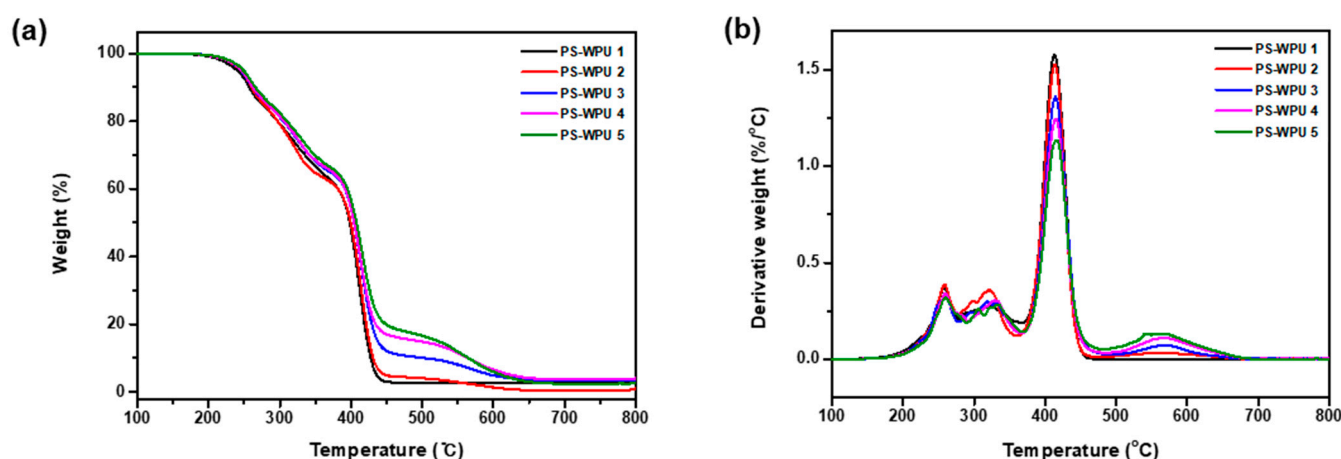


Figure 6. (a) TGA and (b) DTG curves of PS-WPU samples.

Table 4. Thermal properties of PS-WPU samples.

Samples	Decomposition Temperature		
	T _{10%} (°C)	T _{50%} (°C)	T _{max%} (°C)
PS-WPU 1	257.4	398.3	412.7
PS-WPU 2	260.5	399.9	413.7
PS-WPU 3	262.3	404.4	414.8
PS-WPU 4	262.4	404.5	415.7
PS-WPU 5	262.4	407.9	416.8

3.6. Mechanical Properties

The stress–strain curves of the PS-WPU samples are shown in Figure 7, and the obtained values of tensile strength, elongation at break, and modulus are summarized in Table 5. The PS-WPU 1 without PDMS shows a maximum stress of 23.27 MPa, modulus of 4.42 MPa, and strain of 246% at room temperature. Tensile strength and modulus gradually decrease with increasing PDMS content from 23.27 to 10.05 MPa and 4.42 to 0.51 MPa, respectively. However, the strain at break increases from 246 to 434% with increasing PDMS content. As shown in Table 5, a similar trend is observed at -60 °C. With increasing PDMS content, tensile strength and modulus decrease from 32.84 to 20.97 MPa and 11.81 to 3.59 MPa, respectively. The elongation at break increases from 211 to 392%. Interestingly, the obtained tensile strength and modulus values at -60 °C are higher than those obtained at room temperature. The elongation at break is lower at -60 °C than at room temperature. These results indicate that the incorporation of PDMS can improve the flexibility, elasticity, and low temperature properties [31].

Table 5. Mechanical properties of PS-WPU samples.

Samples	Tensile Strength (MPa)		Elongation at Break (%)		Young's Modulus (MPa)	
	25 °C	-60 °C	25 °C	-60 °C	25 °C	-60 °C
	PS-WPU 1	23.27	32.84	246	211	4.42
PS-WPU 2	17.94	28.18	277	223	2.58	7.12
PS-WPU 3	16.01	25.56	335	298	1.89	6.04
PS-WPU 4	13.37	22.84	377	325	1.56	5.82
PS-WPU 5	10.05	20.97	434	392	0.51	3.59

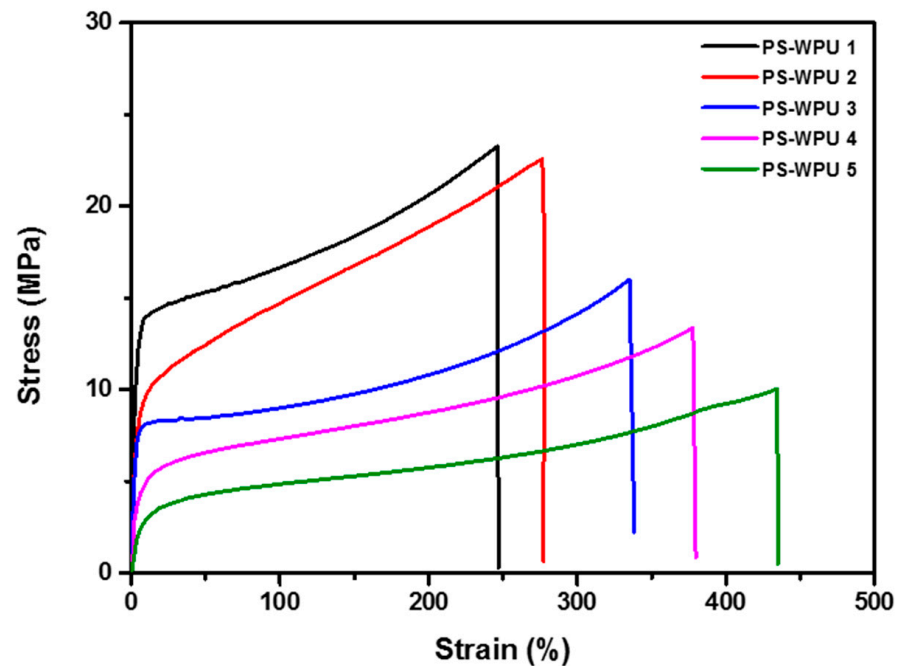


Figure 7. Stress–strain curves of PS-WPU samples obtained at room temperature.

3.7. Surface Hydrophobicity and Water Resistance

The applicability of polymer coating materials can be predicted based on hydrophobicity and water resistance in different testing media. In this study, the hydrophobicity and swelling behavior were investigated using D.W and S.W (5% NaCl). The surface hydrophobicity of the PS-WPU films is investigated by measuring the WCA between the water droplet (D.W and S.W) and the surface of the film, as shown in Figure 8. The surface energy (Table 6) was also calculated from the contact angle values using the Owens equation [48]:

$$\gamma_{SV} = \gamma_{SV}^d + \gamma_{SV}^p$$

$$\gamma_{LV}(1 + \cos\theta_{LV}) = 2\left(\gamma_{LV}^d\gamma_{SV}^d\right)^{1/2} + 2\left(\gamma_{LV}^p\gamma_{SV}^p\right)^{1/2}$$

where γ_{LV} is the surface tension of liquid, θ is the contact angle of liquid on the surface, γ_{LV}^d and γ_{LV}^p are the dispersive and polar components of the liquids, respectively, and γ_{SV}^d and γ_{SV}^p are the dispersive and polar components of the solids, respectively. The dispersion and polar components of water are 21.8 and 51.0 mN/m, respectively. The dispersion and polar components of formamide are 39.0 and 19.0 mN/m, respectively.

The WCAs of the PS-WPU 1 film without PDMS for D.W and S.W are 80.3° and 82.0°, respectively. With increasing PDMS content from 0% to 20%, the WCA for D.W and S.W increases from 80.3° to 101.8° and 82.0° to 99.5°, respectively. In addition, the surface energy of the PS-WPU films decreases with increasing PDMS content for D.W and S.W. For D.W, the surface energy of the PS-WPU films decreases from 34.1 mN/m to 20.9 mN/m with increasing PDMS content. For S.W, the surface energy of the PS-WPU films decreases from 46.6 mN/m to 34.1 mN/m with increasing PDMS content. This result confirms that the incorporation of PDMS can improve the surface hydrophobicity of the copolymers. The presence of siloxane provides a thermodynamic driving force for siloxane segments to migrate toward the air–polymer interface of the film during film formation. As a result, a siloxane-enriched surface is formed, which has a low surface energy because of weak intermolecular forces between the methyl groups (–CH₃) and the strong (Si–O) and flexible (Si–O–Si) siloxane chain [49,50].

Water resistance is an important factor in coating materials. The water resistance of polymers is an attribute of their hydrophobicity, as well as the interaction between macro-

molecules [51,52]. To evaluate the water resistance of the PS-WPU films, the samples were immersed in water (D.W and S.W) for 168 h. The relationship between the water swelling ratio and soaking time of the PS-WPU films is shown in Figure 9a,b. The swelling ratio increases with increased soaking time up to 72 h and then levels off. The water swelling ratio of the PS-WPU films decreases with increasing PDMS content. The improved water resistance may be ascribed to the hydrophobicity of PDMS. When the films are immersed in water, the water fills the microcavities and they swell due to the interaction between the hydrophilic groups and water, resulting in the absorption of water. However, incorporating hydrophobic PDMS creates a hydrophobic barrier on the surface to prevent water absorption and reduce the interaction between hydrophilic groups and water [31,41,53,54]. Thus, it can be concluded that by incorporating hydrophobic PDMS into the soft segment of the PU chains, the water resistance of the PS-WPU films was enhanced. These results suggest that PS-WPUs have potential as coating materials for S.W repellent applications.

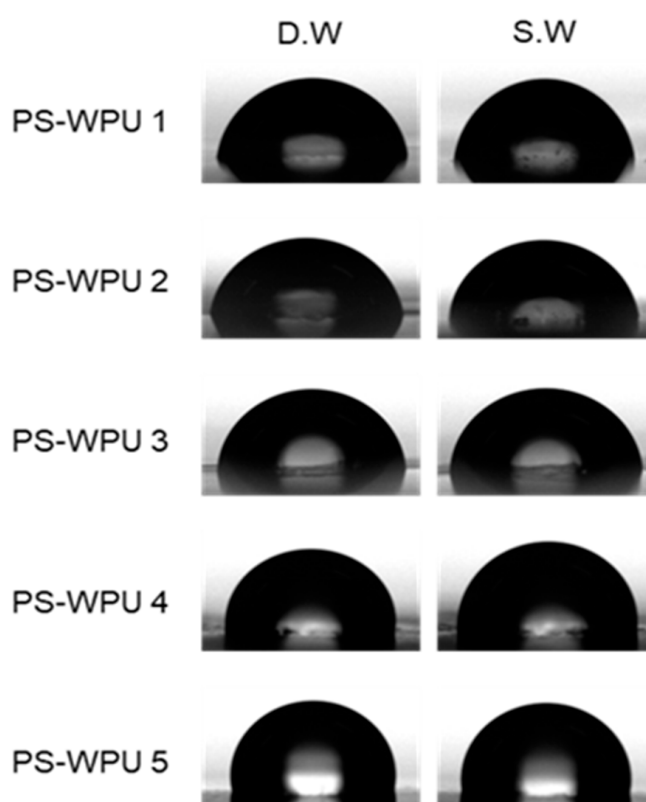


Figure 8. Water contact angles images of the recorded droplets (D.W and S.W) on the surface of PS-WPUs.

Table 6. Performance of the PS-WPU samples.

Samples	Water Contact Angle (°)		Surface Energy (γ) (mN/m)		Maximum Water Absorption (%)	
	D.W	S.W	D.W	S.W	D.W	S.W
PS-WPU 1	80.3	82.0	34.1	46.6	29.2	16.1
PS-WPU 2	83.6	83.9	32.0	45.2	20.0	15.0
PS-WPU 3	85.1	85.6	31.1	44.0	18.5	12.5
PS-WPU 4	95.0	95.0	25.1	37.3	11.5	7.1
PS-WPU 5	101.8	99.5	20.9	34.1	6.9	5.0

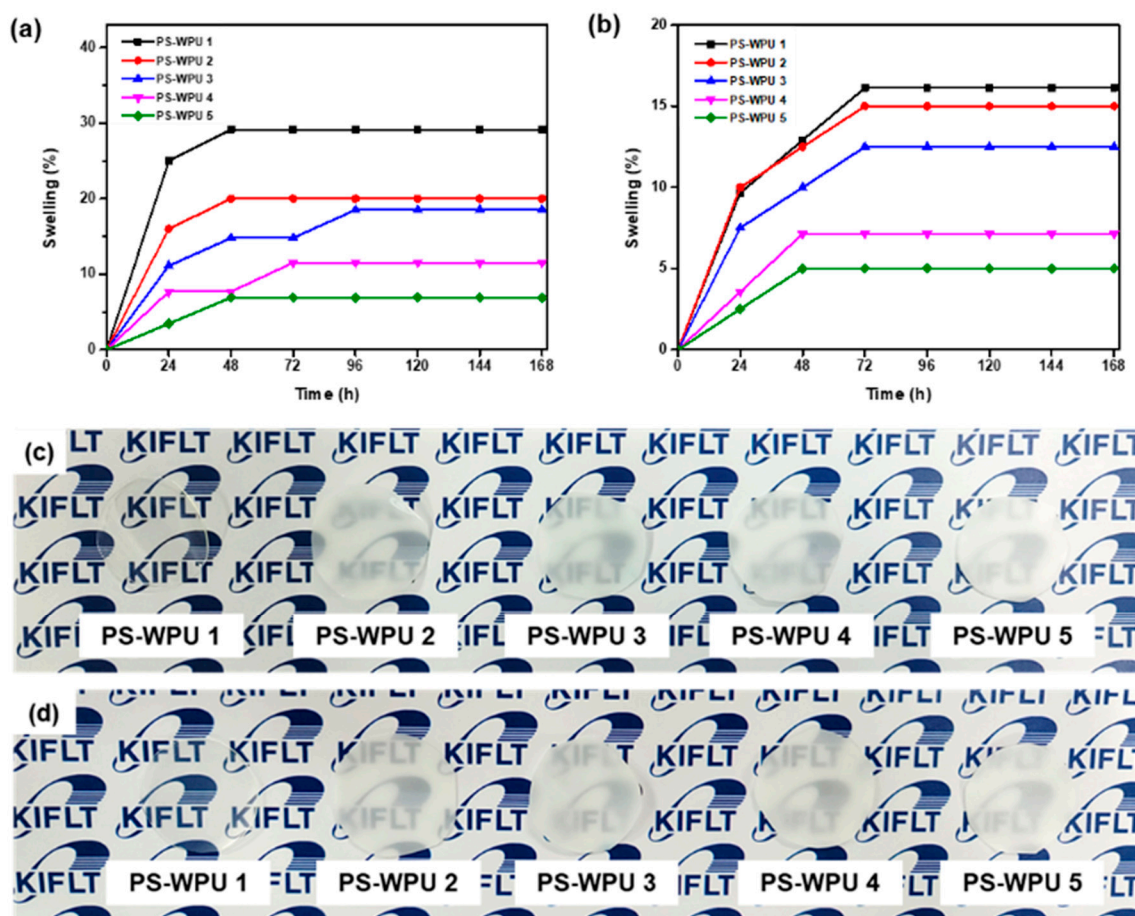


Figure 9. Water swelling ratio of the PS-WPU samples in (a) D.W and (b) S.W Images of the PS-WPU samples (c) before and (d) after swelling in D.W.

4. Conclusions

In this study, a series of PDMS-modified WPU were synthesized with various PDMS contents. FTIR and XPS analyses confirmed the successful incorporation of PDMS into the PU soft segment. The average particle size of the PS-WPU samples increased with increasing PDMS content because of the large free volume and low chain packing density in the interior of the colloidal particles. XRD analysis showed that all the PS-WPU samples were amorphous, and the orientation of the PU chains was disturbed by the PDMS content. DMA results showed that the storage modulus and T_g of the samples decreased with increasing PDMS content. According to the TGA and DTG results, the incorporation of PDMS increased the thermal stability because of the higher energy of Si–O bonds compared to the C–C and C–O bonds. The tensile strength decreased, but the elongation at break increased with increasing PDMS content at 25 °C and –60 °C owing to the flexibility, poor tensile strength, and excellent low temperature properties of PDMS. In addition, the WCA and water resistance results confirmed that both D.W and S.W had good surface hydrophobicity and water resistance. According to all the results, the PS-WPU samples in this study represent excellent candidates for potential use as coatings in marine applications.

Author Contributions: M.-G.K. conceived the research idea. M.-G.K., E.K., J.-W.K. and J.H.L. wrote the main manuscript. M.-G.K., K.-I.J. and J.-H.P. performed the experiments. All authors reviewed the manuscript. All authors have read and agreed to the published version of the manuscript.

Funding: This research received no external funding.

Institutional Review Board Statement: Not applicable.

Informed Consent Statement: Not applicable.

Data Availability Statement: The data presented in this study are available on request from the corresponding author.

Acknowledgments: This research was supported by the Material and Component Development funded by the Korea Evaluation Institute of Industrial Technology (No. 20013166). This research was also supported by the National Research Foundation of Korea (NRF) funded by the MSIT (Grant Numbers. NRF–2019R1G1A1100122). This work was supported by the Technology Innovation Program (Development of modified polyvinylidene fluoride resin for spinning/coating products having MFR > 10 g/10 min, 1415173686, 20015987) funded by the Ministry of Trade, Industry and Energy (MOTIE, Korea).

Conflicts of Interest: The authors declare no conflict of interest.

References

1. Yin, X.; Li, X.; Luo, Y. Synthesis and Characterization of Multifunctional Two-Component Waterborne Polyurethane Coatings: Fluorescence, Thermostability and Flame Retardancy. *Polymers* **2017**, *9*, 492. [[CrossRef](#)] [[PubMed](#)]
2. Wang, F.; Feng, L.; Li, G. Properties of waterborne polyurethane conductive coating with low MWCNTs content by electrostatic spraying. *Polymers* **2018**, *10*, 1406. [[CrossRef](#)]
3. Che, J.-Y.; Cheon, J.-M.; Chun, J.-H.; Park, C.-C.; Lee, Y.-H.; Kim, H.-D. Preparation and properties of emulsifier-/solvent-free slightly crosslinked waterborne polyurethane-acrylic hybrid emulsions for footwear adhesives (III)—effect of trimethylol propane (TMP)/ethylene diamine (EDA) content. *J. Adhes. Sci. Technol.* **2017**, *31*, 1872–1887. [[CrossRef](#)]
4. Cakić, S.M.; Ristić, I.S.; Milena, M.; Stojiljković, D.T.; Jaroslava, B. Preparation and characterization of waterborne polyurethane/silica hybrid dispersions from castor oil polyols obtained by glycolysis poly (ethylene terephthalate) waste. *Int. J. Adhes. Adhes.* **2016**, *70*, 329–341. [[CrossRef](#)]
5. Shi, H.; Shi, D.; Yin, L.; Yang, Z.; Luan, S.; Gao, J.; Zha, J.; Yin, J.; Li, R.K. Ultrasonication assisted preparation of carbonaceous nanoparticles modified polyurethane foam with good conductivity and high oil absorption properties. *Nanoscale* **2014**, *6*, 13748–13753. [[CrossRef](#)] [[PubMed](#)]
6. Li, X.; Fang, Z.; Li, X.; Tang, S.; Zhang, K.; Guo, K. Synthesis and application of a novel bio-based polyol for preparation of polyurethane foams. *N. J. Chem.* **2014**, *38*, 3874–3878. [[CrossRef](#)]
7. Behera, P.K.; Usha, K.; Guchhait, P.; Jehnichen, D.; Das, A.; Voit, B.; Singha, N.K. A novel ionomeric polyurethane elastomer based on ionic liquid as crosslinker. *RSC Adv.* **2016**, *6*, 99404–99413. [[CrossRef](#)]
8. Tang, D.; Macosko, C.W.; Hillmyer, M.A. Thermoplastic polyurethane elastomers from bio-based poly (δ -decalactone) diols. *Polym. Chem.* **2014**, *5*, 3231–3237. [[CrossRef](#)]
9. Nelson, A.M.; Long, T.E. Synthesis, properties, and applications of ion-containing polyurethane segmented copolymers. *Macromol. Chem. Phys.* **2014**, *215*, 2161–2174. [[CrossRef](#)]
10. Chattopadhyay, D.K.; Raju, K. Structural engineering of polyurethane coatings for high performance applications. *Prog. Polym. Sci.* **2007**, *32*, 352–418. [[CrossRef](#)]
11. Jaudouin, O.; Robin, J.J.; Lopez-Cuesta, J.M.; Perrin, D.; Imbert, C. Ionomer-based polyurethanes: A comparative study of properties and applications. *Polym. Int.* **2012**, *61*, 495–510. [[CrossRef](#)]
12. Florian, P.; Jena, K.K.; Allauddin, S.; Narayan, R.; Raju, K. Preparation and characterization of waterborne hyperbranched polyurethane-urea and their hybrid coatings. *Ind. Eng. Chem. Res.* **2010**, *49*, 4517–4527. [[CrossRef](#)]
13. Chen, G.N.; Chen, K.N. Hybridization of aqueous-based polyurethane with glycidyl methacrylate copolymer. *J. Appl. Polym. Sci.* **1999**, *71*, 903–913. [[CrossRef](#)]
14. Wang, A.A.; Lee, K.-R.; Hsu, T.-N.; Wang, D.-M.; Lai, J.-Y. 2, 3-(Epoxypropyl)-methacrylate chemical modified polyurethane membrane for pervaporation. *Eur. Polym. J.* **1998**, *34*, 1105–1111. [[CrossRef](#)]
15. Xie, D.-Y.; Song, F.; Zhang, M.; Wang, X.-L.; Wang, Y.-Z. Roles of soft segment length in structure and property of soy protein isolate/waterborne polyurethane blend films. *Ind. Eng. Chem. Res.* **2016**, *55*, 1229–1235. [[CrossRef](#)]
16. Awad, S.; Chen, H.; Chen, G.; Gu, X.; Lee, J.L.; Abdel-Hady, E.; Jean, Y. Free volumes, glass transitions, and cross-links in zinc oxide/waterborne polyurethane nanocomposites. *Macromolecules* **2011**, *44*, 29–38. [[CrossRef](#)]
17. Zhang, L.; Zhang, H.; Guo, J. Synthesis and properties of UV-curable polyester-based waterborne polyurethane/functionalized silica composites and morphology of their nanostructured films. *Ind. Eng. Chem. Res.* **2012**, *51*, 8434–8441. [[CrossRef](#)]
18. Zhao, J.; Zhou, T.; Zhang, J.; Chen, H.; Yuan, C.; Zhang, W.; Zhang, A.E.C. Synthesis of a waterborne polyurethane-fluorinated emulsion and its hydrophobic properties of coating films. *Ind. Eng. Chem. Res.* **2014**, *53*, 19257–19264. [[CrossRef](#)]
19. Lu, Y.; Larock, R.C. New hybrid latexes from a soybean oil-based waterborne polyurethane and acrylics via emulsion polymerization. *Biomacromolecules* **2007**, *8*, 3108–3114. [[CrossRef](#)]
20. Pergal, M.; Džunuzović, J.; Poreba, R.; Micic, D.; Stefanov, P.; Pezo, L.; Spirkova, M. Surface and thermomechanical characterization of polyurethane networks based on poly (dimethylsiloxane) and hyperbranched polyester. *Express Polym. Lett.* **2013**, *7*, 806–820. [[CrossRef](#)]

21. Yen, M.-S.; Tsai, P.-Y.; Hong, P.-D. The solution properties and membrane properties of polydimethylsiloxane waterborne polyurethane blended with the waterborne polyurethanes of various kinds of soft segments. *Colloids Surf. A Physicochem. Eng.* **2006**, *279*, 1–9. [[CrossRef](#)]
22. Li, Y.-Q.; Zhu, W.-B.; Yu, X.-G.; Huang, P.; Fu, S.-Y.; Hu, N.; Liao, K. Multifunctional wearable device based on flexible and conductive carbon sponge/polydimethylsiloxane composite. *ACS Appl. Mater. Interfaces* **2016**, *8*, 33189–33196. [[CrossRef](#)] [[PubMed](#)]
23. Planes, M.; Brand, J.; Lewandowski, S.; Remaury, S.; Solé, S.; Le Coz, C.; Carlotti, S.; Sèbe, G. Improvement of the Thermal and Optical Performances of Protective Polydimethylsiloxane Space Coatings with Cellulose Nanocrystal Additives. *ACS Appl. Mater. Interfaces* **2016**, *8*, 28030–28039. [[CrossRef](#)] [[PubMed](#)]
24. Dundua, A.; Franzka, S.; Ulbricht, M. Improved antifouling properties of polydimethylsiloxane films via formation of polysiloxane/polyzwitterion interpenetrating networks. *Macromol. Rapid Commun.* **2016**, *37*, 2030–2036. [[CrossRef](#)] [[PubMed](#)]
25. Chen, J.; Guo, H.; Ding, P.; Pan, R.; Wang, W.; Xuan, W.; Wang, X.; Jin, H.; Dong, S.; Luo, J. Transparent triboelectric generators based on glass and polydimethylsiloxane. *Nano Energy* **2016**, *30*, 235–241. [[CrossRef](#)]
26. Vlad, S.; Vlad, A.; Oprea, S. Interpenetrating polymer networks based on polyurethane and polysiloxane. *Eur. Polym. J.* **2002**, *38*, 829–835. [[CrossRef](#)]
27. Zheng, G.; Lu, M.; Rui, X.J.A.S.S. The effect of polyether functional polydimethylsiloxane on surface and thermal properties of waterborne polyurethane. *Eur. Polym. J.* **2017**, *399*, 272–281. [[CrossRef](#)]
28. Xu, C.-A.; Lu, M.; Wu, K.; Shi, J. Effects of Polyether and Polyester Polyols on the Hydrophobicity and Surface Properties of Polyurethane/Polysiloxane Elastomers. *Macromol. Res.* **2020**, *28*, 1032–1039. [[CrossRef](#)]
29. Lin, Y.; Yi, P.; Yu, M.; Li, G. Fabrication and performance of a novel 3D superhydrophobic material based on a loofah sponge from plant. *Mater. Lett.* **2018**, *230*, 219–223. [[CrossRef](#)]
30. Seymour, R.; Estes, G.; Cooper, S.L. Infrared studies of segmented polyurethane elastomers. I. Hydrogen bonding. *Macromolecules* **1970**, *3*, 579–583. [[CrossRef](#)]
31. Zhang, C.; Zhang, X.; Dai, J.; Bai, C. Synthesis and properties of PDMS modified waterborne polyurethane–Acrylic hybrid emulsion by solvent-free method. *Prog. Org. Coat.* **2008**, *63*, 238–244. [[CrossRef](#)]
32. Lee, S.W.; Lee, Y.H.; Park, H.; Do Kim, H. Effect of total acrylic/fluorinated acrylic monomer contents on the properties of waterborne polyurethane/acrylic hybrid emulsions. *Macromol. Res.* **2013**, *21*, 709–718. [[CrossRef](#)]
33. Chen, R.S.; Chang, C.J.; Chang, Y.H. Study on siloxane-modified polyurethane dispersions from various polydimethylsiloxanes. *J. Polym. Sci. A Polym. Chem.* **2005**, *43*, 3482–3490. [[CrossRef](#)]
34. Nanda, A.K.; Wicks, D.A. The influence of the ionic concentration, concentration of the polymer, degree of neutralization and chain extension on aqueous polyurethane dispersions prepared by the acetone process. *Polymers* **2006**, *47*, 1805–1811. [[CrossRef](#)]
35. Wang, L.; Shen, Y.; Lai, X.; Li, Z.; Liu, M. Synthesis and properties of crosslinked waterborne polyurethane. *J. Polym. Res.* **2011**, *18*, 469–476. [[CrossRef](#)]
36. Zhang, T.; Xi, K.; Yu, X.; Gu, M.; Guo, S.; Gu, B.; Wang, H. Synthesis, properties of fullerene-containing polyurethane–urea and its optical limiting absorption. *Polymers* **2003**, *44*, 2647–2654. [[CrossRef](#)]
37. Hernandez, R.; Weksler, J.; Padsalgikar, A.; Runt, J. Microstructural organization of three-phase polydimethylsiloxane-based segmented polyurethanes. *Macromolecules* **2007**, *40*, 5441–5449. [[CrossRef](#)]
38. Głowińska, E.; Datta, J. Structure, morphology and mechanical behaviour of novel bio-based polyurethane composites with microcrystalline cellulose. *Cellulose* **2015**, *22*, 2471–2481. [[CrossRef](#)]
39. Wang, Y.; Qiu, F.; Xu, B.; Xu, J.; Jiang, Y.; Yang, D.; Li, P. Preparation, mechanical properties and surface morphologies of waterborne fluorinated polyurethane-acrylate. *Prog. Org. Coat.* **2013**, *76*, 876–883. [[CrossRef](#)]
40. Yi, T.; Ma, G.; Hou, C.; Li, S.; Zhang, R.; Wu, J.; Hao, X.; Zhang, H. Polyurethane-acrylic hybrid emulsions with high acrylic/polyurethane ratios: Synthesis, characterization, and properties. *J. Appl. Polym. Sci.* **2017**, *134*, 44488. [[CrossRef](#)]
41. Yi, T.; Ma, G.; Hou, C.; Li, S.; Zhang, R.; Wu, J.; Hao, X. Preparation and properties of poly (siloxane-ether-urethane)-acrylic hybrid emulsions. *J. Appl. Polym. Sci.* **2017**, *134*, 44927. [[CrossRef](#)]
42. Hassanajili, S.; Khademi, M.; Keshavarz, P. Influence of various types of silica nanoparticles on permeation properties of polyurethane/silica mixed matrix membranes. *J. Membr. Sci.* **2014**, *453*, 369–383. [[CrossRef](#)]
43. Ren, N.; Song, Y.; Tao, C.; Cong, B.; Cheng, Q.; Huang, Y.; Xu, G.; Bao, J. Effect of the soft and hard segment composition on the properties of waterborne polyurethane-based solid polymer electrolyte for lithium ion batteries. *J. Solid State Electrochem.* **2018**, *22*, 1109–1121. [[CrossRef](#)]
44. Bahadur, A.; Saeed, A.; Iqbal, S.; Shoaib, M.; ur Rahman, M.S.; Bashir, M.I.; Asghar, M.; Ali, M.A.; Mahmood, T. Biocompatible waterborne polyurethane-urea elastomer as intelligent anticancer drug release matrix: A sustained drug release study. *React. Funct. Polym.* **2017**, *119*, 57–63. [[CrossRef](#)]
45. Stefanović, I.S.; Špirková, M.; Ostojić, S.; Stefanov, P.; Pavlović, V.B.; Pergal, M.V. Montmorillonite/poly (urethane-siloxane) nanocomposites: Morphological, thermal, mechanical and surface properties. *Appl. Clay Sci.* **2017**, *149*, 136–146. [[CrossRef](#)]
46. Yilgör, E.; Yilgör, I. Silicone containing copolymers: Synthesis, properties and applications. *Prog. Polym. Sci.* **2014**, *39*, 1165–1195. [[CrossRef](#)]

47. Stefanović, I.S.; Džunuzović, J.V.; Džunuzović, E.S.; Brzić, S.J.; Jasiukaitytė-Grojzdek, E.; Basagni, A.; Marega, C. Tailoring the properties of waterborne polyurethanes by incorporating different content of poly (dimethylsiloxane). *Prog. Org. Coat.* **2021**, *161*, 106474. [[CrossRef](#)]
48. Yu, F.; Xu, X.; Lin, N.; Liu, X.Y. Structural engineering of waterborne polyurethane for high performance waterproof coatings. *RSC Adv.* **2015**, *5*, 72544–72552. [[CrossRef](#)]
49. Joki-Korpela, F.; Pakkanen, T.T. Incorporation of polydimethylsiloxane into polyurethanes and characterization of copolymers. *Eur. Polym. J.* **2011**, *47*, 1694–1708. [[CrossRef](#)]
50. Ge, Z.; Luo, Y. Synthesis and characterization of siloxane-modified two-component waterborne polyurethane. *Prog. Org. Coat.* **2013**, *76*, 1522–1526. [[CrossRef](#)]
51. Wang, G.; Ma, G.; Hou, C.; Guan, T.; Ling, L.; Wang, B. Preparation and properties of waterborne polyurethane/nanosilica composites: A diol as extender with triethoxysilane group. *J. Appl. Polym. Sci.* **2014**, *131*, 40526. [[CrossRef](#)]
52. Ma, G.; Guan, T.; Hou, C.; Wu, J.; Wang, G.; Ji, X.; Wang, B. Research. Preparation, properties and application of waterborne hydroxyl-functional polyurethane/acrylic emulsions in two-component coatings. *J. Coat. Technol. Res.* **2015**, *12*, 505–512. [[CrossRef](#)]
53. Džunuzović, J.V.; Pergal, M.V.; Poreba, R.; Vodnik, V.V.; Simonović, B.R.; Špírková, M.; Jovanović, S. Analysis of dynamic mechanical, thermal and surface properties of poly (urethane-ester-siloxane) networks based on hyperbranched polyester. *J. NonCryst. Solids* **2012**, *358*, 3161–3169. [[CrossRef](#)]
54. Wang, L.; Maruf, S.H.; Maniglio, D.; Ding, Y. Fabrication and characterizations of crosslinked porous polymer films with varying chemical compositions. *Polymers* **2012**, *53*, 3749–3755. [[CrossRef](#)]